

Self-energy correction to the energy levels of heavy muonic atoms

Natalia S. Oreshkina *

Max-Planck-Institut für Kernphysik, Saupfercheckweg 1, 69117 Heidelberg, Germany

 (Received 3 June 2022; revised 5 August 2022; accepted 28 September 2022; published 30 November 2022)

The fully relativistic, rigorous QED calculations of the self-energy correction to the fine-structure levels of heavy muonic atoms are reported, including rigorous predictions for excited states. We discuss nuclear model and parameter dependence for this contribution as well as numerical convergence issues. The presented results mostly agree with previously reported estimations, with some exceptions, including ones used for the determination of the nuclear root-mean-square radii, and underline the importance of rigorous QED calculations for the theoretical prediction of the spectra of muonic atoms.

DOI: [10.1103/PhysRevResearch.4.L042040](https://doi.org/10.1103/PhysRevResearch.4.L042040)

Introduction. Muonic atoms are the bound systems of an atomic nucleus and a negatively charged muon. Being more than 200 times heavier than an electron, a muon possesses correspondingly downscaled atomic orbitals radii, which in the case of heavy muonic atoms are comparable or even smaller than the nuclear radius. This leads to huge finite-nuclear-size effects and a strong dependence of the muon's bound-state energies on the nuclear charge and current distributions, as well as to large relativistic effects. The understanding of this strong dependence of the muonic atoms on nuclear parameters, and the information about atomic nuclei that they can deliver, has triggered interest in precise knowledge of the level structure of muonic atoms [1–3]. A combination of state-of-the-art theoretical predictions of the level structure and experiments measuring the transition energies in muonic atoms enabled the determination of nuclear parameters like nuclear-charge or root-mean-square (rms) radii [4–7], electric quadrupole, and magnetic dipole moments [8–11]. One of the most precise measurements to date is the determination of the rms radius of ^{208}Pb to a 0.02% level [12].

The short lifetime of muon leads to the fact that muonic atoms are essentially muonic hydrogenlike and can be described with the single-particle Dirac equation. The theory of muonic atoms, including nuclear and leading quantum electrodynamics (QED) corrections, has been presented already in Refs. [2,13]. Recently the updated state-of-the-art calculations of the fine and hyperfine structures of heavy muonic atoms and the corresponding analysis of the individual contributions has been presented in Refs. [14–18]. One of the important effects is the self-energy (SE) correction. Unlike the case of atomic electrons, where SE is comparable to another QED correc-

tion, the vacuum polarization (VP) correction [19], in muonic atoms the VP correction is by far the dominant one [2]. Therefore, the SE correction is much smaller than the leading VP correction and was previously calculated within a relatively simple mean-value evaluation method, suggested in Ref. [20] and later used in Refs. [2,21]. Later, an attempt at a more precise calculation was made in Ref. [22] for the ground $1s_{1/2}$ state of several muonic atoms with a final uncertainty of about 5%. However, even most recent works on muonic atoms still treat the leading VP correction as the total QED contribution, excluding SE [7] or estimating it to be very small [17].

Additionally, in some cases the analysis of high-precision spectroscopic x-ray measurements of the muonic transitions revealed some anomalies and disagreements with theoretical predictions. Thus the assumption about the most complicated nuclear polarization (NP) correction deduced from the experimental data for fine-structure components difference $\Delta 2p = E_{2p_{3/2}} - E_{2p_{1/2}}$ had an opposite sign compared to the theory results for ^{90}Zr [23], $^{112-124}\text{Sn}$ [5], and ^{208}Pb [12,24]. For a long time, it was believed that this so-called fine-structure anomaly can be explained by more precise predictions on the NP correction, but recently this was shown not to be the case [25] and, therefore, additional attention should be paid to other contributions, in particular to the last remaining sizable QED effect, namely, to the SE correction.

In this Letter, we present rigorous, fully relativistic QED calculations of the SE correction to the ground $1s_{1/2}$ and excited $2p_{1/2}$ and $2p_{3/2}$ state energies of muonic atoms, and establish the accuracy of our predictions for several muonic atoms of interest. The results can be used for future experiments aiming at high-precision determination of nuclear rms radii and for reanalyzing the existing experimental data in order to resolve the fine-structure anomaly.

Formalism. The method for calculation of the SE correction for a bound electron in highly charged hydrogenlike ions was first proposed in Ref. [26], used in Ref. [27], and further improved in Refs. [28,29]. In our current work, we apply the procedure described in detail in [30,31] with an emphasis on the finite-nuclear size effects.

*Natalia.Oreshkina@mpi-hd.mpg.de

The self-energy correction to the state a with energy ε_a can be written in terms of the matrix element of $\Sigma(E)$ in the Feynman gauge as [30,31]

$$\langle a|\Sigma(\varepsilon_a)|a\rangle = \frac{i}{2\pi} \int_{-\infty}^{\infty} d\omega \sum_n \frac{\langle an|I(\omega)|na\rangle}{\varepsilon_a - \omega - \varepsilon_n(1 - i0)}, \quad (1)$$

$$I(\omega, \mathbf{x}_1, \mathbf{x}_2) = \alpha \frac{(1 - \alpha_1 \alpha_2) \exp(i\sqrt{\omega^2 + i0}x_{12})}{x_{12}}. \quad (2)$$

Here, x_{12} is the relative distance $x_{12} = |\mathbf{x}_1 - \mathbf{x}_2|$, α are the Dirac matrices, ω is the energy of a virtual photon, and the summation goes over the full spectrum n of the considered lepton (electron or muon), including negative- and positive-energy states. The muonic relativistic system of units ($\hbar = m_\mu = c = 1$) and Heaviside charge units [$\alpha = e^2/(4\pi)$] are used throughout the paper. Bold letters are used for three-vectors; the components of three-vectors are listed with Latin indices, whereas Greek letters denote four-vector indices. The usage of the relativistic muonic system of units with $m_\mu = 1$ allows us to use exactly the same formulas which were derived for electronic atoms in the relativistic electronic system of units with $m_e = 1$, and the difference appears only in the value of the rms radius.

Following the procedure and notations from Refs. [30,31], we expand the Green's function for the bound muon in powers of the Coulomb potential as the sum of zero-potential, one-potential, and many-potential terms. After performing the angular integration analytically, one can write the total SE correction for a state a as the sum of corresponding nondivergent terms as

$$\Delta E_a^{\text{SE}} = \Delta E_a^{(0)} + \Delta E_a^{(1)} + \Delta E_a^{(2+)}. \quad (3)$$

The zero-potential term is calculated in the momentum representation as the diagonal SE matrix element:

$$\Delta E_a^{(0)} = \frac{\alpha}{4\pi} \int_0^\infty \frac{dp p^2}{(2\pi)^3} \{a(\rho)(g_a^2 - f_a^2) + b(\rho)[\varepsilon_a(g_a^2 + f_a^2) + 2p g_a f_a]\}, \quad (4)$$

where g_a and f_a are large and small components of the radial wave function of the state a with the energy ε_a in the momentum representation, $\rho = 1 - p^2[(e^2 + p^2)]$, and the functions $a(\rho)$ and $b(\rho)$ are given in Ref. [31].

The one-potential term has one single interaction between the muon and the nucleus inside the SE loop, and its final renormalized expression can be written in the momentum representation as [30–32]

$$\Delta E_a^{(1)} = \frac{\alpha}{2(2\pi)^6} \int_0^\infty dp p^2 \int_0^\infty dp' p'^2 \times \int_{-1}^1 d\xi V(q) [\mathcal{F}_1^{aa} P_l(\xi) + \mathcal{F}_2^{aa} P_l(\xi)], \quad (5)$$

where $q^2 = p^2 + p'^2 - 2pp'\xi$, \bar{l} is defined through the total angular momentum j and orbital angular momentum l as $\bar{l} = 2j - l$, P_l are the Legendre polynomials, and $\mathcal{F}_{1,2}^{ab}$ contain one more internal integration and are given in Ref. [31]. The exact expressions for the nuclear potential $V(q)$ in the momentum representation will be discussed later.

Finally, the many-potential term with two or more interactions between the muon and the nucleus inside the SE loop can

be calculated in the coordinate representation, and performing the angular integrations and summations analytically one gets

$$\Delta E_a^{(2+)} = \frac{i\alpha}{2\pi} \int_{-\infty}^{\infty} d\omega \sum_{nJ} \frac{(-1)^{j_n - j_a + J}}{2j_a + 1} \times \frac{R_J(\omega, an'n'a)}{\varepsilon_a - \omega - \varepsilon_n(1 - i0)}, \quad (6)$$

where ω corresponds to the energy of the virtual photon, $R_J(\omega, abcd)$ are generalized Slater radial integrals [31], the sum over n in this expression corresponds to the summation over the intermediate states, and

$$|n'\rangle = \sum_f \frac{|f\rangle\langle f|V|n\rangle}{\varepsilon_a - \omega - \varepsilon_f(1 - i0)}. \quad (7)$$

Here $|n\rangle$ is a bound state in the external nuclear potential V and $|f\rangle$ belongs to the spectrum of the free muon.

Nuclear potentials in coordinate and momentum representations. In addition to the wave function in the momentum representation for the calculation of zero- and one-potential terms (4) and (5), one-potential contribution also contains the nuclear potential. Calculated with a generalized Fourier transform [31], the Coulomb potential for pointlike nucleus

$$V_{\text{Coul}}(r) = -\frac{\alpha Z}{r} \quad (8)$$

has the following view in the momentum representation:

$$V_{\text{Coul}}(q) = -4\pi \frac{\alpha Z}{q^2}. \quad (9)$$

However, the Coulomb potential should not be applied in the case of muonic atoms due to the significant nuclear effects and therefore in the current work it has been replaced with different finite-nuclear-size potentials. The first of them, the shell distribution model, has a simple analytical form in both coordinate and momentum representations:

$$V_{\text{shell}}(r) = \begin{cases} -\frac{\alpha Z}{R_0}, & r < R_0, \\ -\frac{\alpha Z}{r}, & r > R_0, \end{cases} \quad (10)$$

$$V_{\text{shell}}(q) = -4\pi \frac{\alpha Z \sin R_0 q}{q^2 R_0 q}. \quad (11)$$

Here, the parameter R_0 is defined in terms of the rms radius as $R_0 = \sqrt{\langle r^2 \rangle}$. A nuclear model which assumes homogeneous-sphere charge distribution of the charge density corresponds to the following potential in the coordinate and momentum representations:

$$V_{\text{sph}}(r) = \begin{cases} -\frac{\alpha Z}{R_0} \left[\frac{3}{2} - \frac{1}{2} \left(\frac{r}{R_0} \right)^2 \right], & r < R_0, \\ -\frac{\alpha Z}{r}, & r > R_0, \end{cases} \quad (12)$$

$$V_{\text{sph}}(q) = -4\pi \frac{\alpha Z}{q^2} \frac{3(\sin R_0 q - R_0 q \cos R_0 q)}{(R_0 q)^3}. \quad (13)$$

The parameter R_0 is now defined as $R_0 = \sqrt{5/3 \langle r^2 \rangle}$. Finally, we also used the most realistic Fermi distribution of the

nuclear density [33]:

$$\rho = \frac{\rho_0}{1 + e^{(r-c)/a}}. \quad (14)$$

Here, a is the skin thickness and it is usually assumed to be $a = 2.3 \text{ fm}/4 \log(3)$ [19,33]. The condition that $V(r)$ has to

be normalized to the nuclear charge Z defines normalization constant ρ_0 and the half-density radius c is chosen to reproduce the rms value.

The analytical formula for the nuclear potential created by Fermi nuclear charge distribution is then [33]

$$V_{\text{Fermi}}(r < c) = -\frac{\alpha Z}{r} \frac{1}{N_{\text{Fermi}}} \left\{ 6 \left(\frac{a}{c} \right)^3 \left[S_3 \left(\frac{r-c}{a} \right) - S_3 \left(-\frac{c}{a} \right) \right] + \frac{r}{c} \left[\frac{3}{2} + \frac{\pi^2}{2} \left(\frac{a}{c} \right)^2 - 3 \left(\frac{a}{c} \right)^2 S_2 \left(\frac{r-c}{a} \right) \right] - \frac{1}{2} \left(\frac{r}{c} \right)^3 \right\}, \quad (15a)$$

$$V_{\text{Fermi}}(r > c) = -\frac{\alpha Z}{r} \frac{1}{N_{\text{Fermi}}} \left\{ N_{\text{Fermi}} + 6 \left(\frac{a}{c} \right)^3 S_3 \left(\frac{c-r}{a} \right) + 3 \left(\frac{a}{c} \right)^2 \frac{r}{c} S_2 \left(\frac{c-r}{a} \right) \right\}, \quad (15b)$$

$$\text{where } S_k(x) = \sum_{n=1}^{\infty} \frac{(-1)^n}{k^n} \exp(nx), \quad N_{\text{Fermi}} = 1 + \pi^2 \left(\frac{a}{c} \right)^2 - 6 \left(\frac{a}{c} \right)^3 S_3 \left(-\frac{c}{a} \right). \quad (15c)$$

After performing a Fourier transform and calculating the integral analytically, we get

$$V_{\text{Fermi}}(q) = V_{\text{Coul}}(q) \left(1 + \frac{\tilde{V}_{\text{triv}}(q)}{N_{\text{Fermi}}} + \frac{\tilde{V}_{\text{sum}}(q)}{N_{\text{Fermi}}} \right), \quad (16a)$$

$$\tilde{V}_{\text{triv}}(q) = -\frac{c^2 + a^2 \pi^2}{c^2} + \frac{1}{(cq)^2} \left(\frac{a^2 q^2 \pi^2 - 6}{2} \cos(cq) + \frac{a^2 q^2 \pi^2 + 6 \sin(cq)}{2 cq} \right), \quad (16b)$$

$$\begin{aligned} \tilde{V}_{\text{sum}}(q) = & 6 \left(\frac{a}{c} \right)^2 \cos(cq) \left[\frac{1}{2(aq)^2} + \frac{\pi^2}{6} - \frac{\pi}{2(aq)} \coth(\pi aq) \right] + 6 \left(\frac{a}{c} \right)^2 \frac{\sin(cq)}{cq} \left[-\frac{1}{2(aq)^2} + \frac{\pi^2}{6} + \frac{\pi^2}{2} \frac{1}{\sinh^2(\pi aq)} \right] \\ & + 6 \left(\frac{a}{c} \right)^3 (aq)^2 \sum_{n=1}^{\infty} \frac{2n^2 + (aq)^2}{n^3 [n^2 + (aq)^2]^2} \exp(-nc/a). \end{aligned} \quad (16c)$$

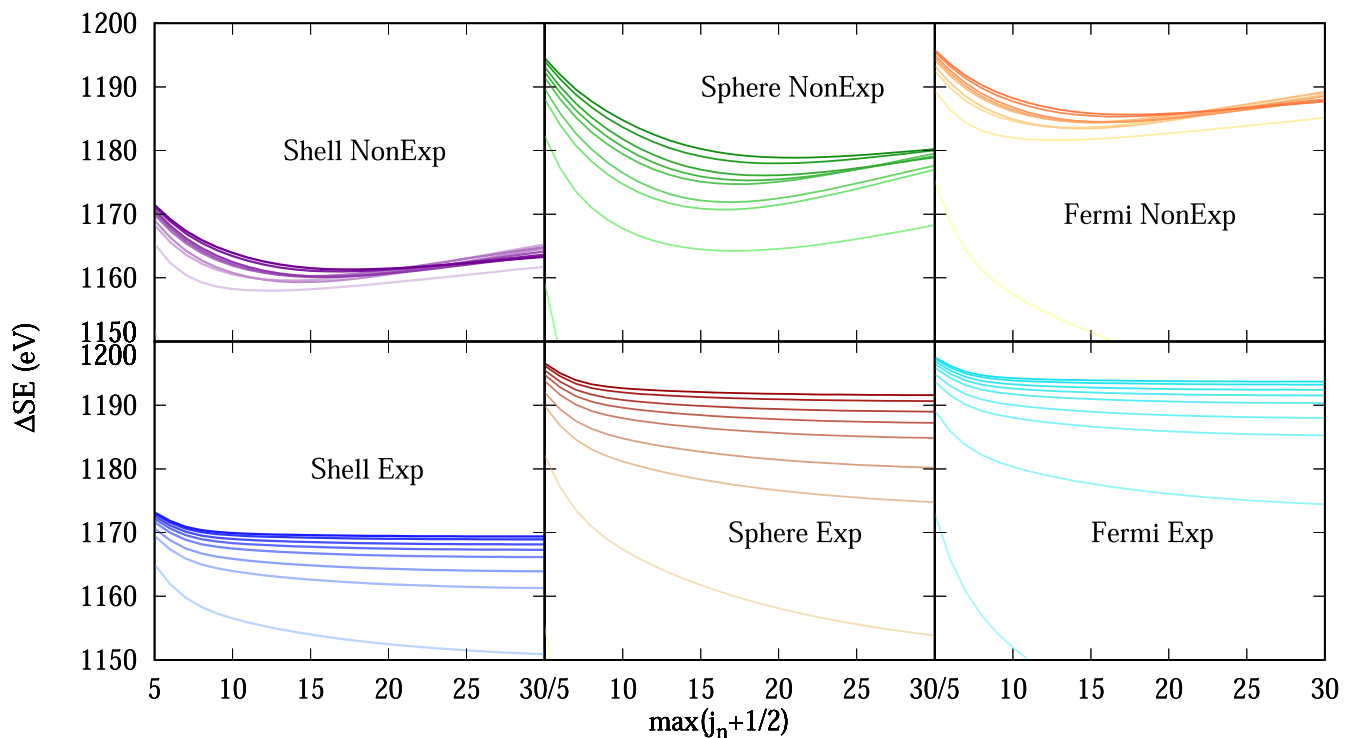


FIG. 1. ΔE_{SE} contribution to the $1s_{1/2}$ state of the muonic zirconium in units of eV as a function of maximal intermediate angular momentum j_n for different nuclear models and numerical grids. The colors of the lines on every panel change depending on the number of used DKB basis functions from light for $n_{\text{DKB}} = 50$ to dark for $n_{\text{DKB}} = 150$.

The only singular contribution in Eq. (16) coincides with the Coulomb part $V_{\text{Coul}}(q)$; all remaining coefficients and contributions are regular at $q = 0$ even though it can be not obvious from the expressions. The potential itself is given in terms of elementary functions and can be easily implemented for numerical calculation with the single exception of the last term in Eq. (16c), which nevertheless converges very fast and therefore does not limit the numerical accuracy.

Calculation details. For the numerical integrations we used the numerical solution of the Dirac equation utilizing the dual-kinetic-basis (DKB) approach [34] involving basis functions represented by piecewise polynomials on grid's intervals from B-splines. This method allows one to find solutions of the Dirac equation for an arbitrary spherically symmetric potential in a finite-size cavity and describes both the discrete and continuous spectra with a finite number of muonic states for every given j and l .

For the numerical evaluation in Eqs. (4) and (5), routines from the numerical integration library QUADPACK [35] have been used for the generalized Fourier transformation of the wave functions and further integrations, following the methods developed in [31]. Analytical formulas (11), (13), and (16) for the nuclear potential in momentum representation have been used for the shell, sphere, and Fermi models, correspondingly.

The summation in the remaining many-potential term over the intermediate state n in Eq. (6) goes over the principal quantum number and at the same time involves an infinite summation over the total angular momentum j_n . Ideally, the calculations with infinite number of basis functions and with the summation which extends up to $j_n = \infty$ would give the most accurate result, but in reality reaching infinity in both of these directions is neither possible nor necessarily beneficial. The DKB wave functions of low-lying bound states are reproduced with very high accuracy and the summations over the Dirac spectrum can be performed very well. However, for the states with high values of angular momentum j even the lowest-lying states have large numbers of knots and oscillate, and therefore the accuracy of the calculations cannot be improved by a simple increase of the basis. Therefore, in our numerical calculations, the individual terms up to the maximum value $j_n + 1/2 = 30$ have been calculated to analyze the convergence. Additionally, for every nuclear model (shell, sphere, and Fermi) and for two different types of the DKB grid (exponential and nonexponential) it has been performed for the number of basic functions n_{DKB} increasing from 50 up to 150.

The corresponding results for the $1s_{1/2}$ state of muonic zirconium are presented in Fig. 1 and for the $2p_{1/2}$ state of muonic tin and $2p_{3/2}$ state of the muonic lead in Fig. 2. The colors of the lines on every panel change from light to dark for lower to higher number of basis functions. As one can see from the figure, the convergence is better for the exponential grid since the results are stable with respect to the maximal j_n , whereas for the nonexponential grid, even though the lines corresponding to the different n_{DKB} are closer to each other, they still change visibly as functions of j_n . The calculated SE correction is rather sensitive to the maximum value j_n , the number of used basic functions n_{DKB} , the nuclear model, and the integration grid, so only a combined deep analysis of these

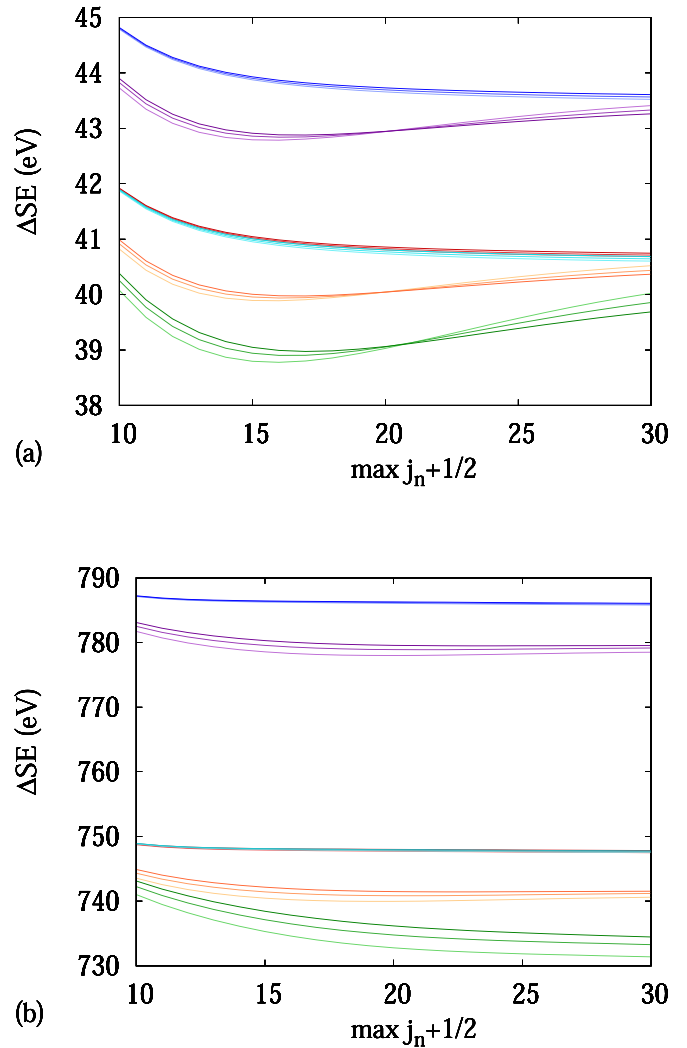


FIG. 2. ΔE_{SE} contribution to the $2p_{1/2}$ state of muonic tin (a) and $2p_{3/2}$ state of the muonic lead (b) in units of eV as a function of maximal intermediate angular momentum j_n for different nuclear models and numerical grids. The color scheme in respect to the nuclear models and numerical grids corresponds to the one used in Fig. 1; the colors of the lines change depending on the number of used DKB basis functions from light for $n_{\text{DKB}} = 130$ to dark for $n_{\text{DKB}} = 150$.

dependencies would allow us to give a reliable and accurate prediction of the effect.

Results. In our current work, we focus on the low-lying states with high importance for experimental analysis for the muonic atoms whose spectra have already been measured before. The total value of the SE correction for the $1s_{1/2}$, $2p_{1/2}$, and $2p_{3/2}$ states of muonic zirconium, tin, and lead for three nuclear models and two DKB grids are listed in Table I, for $\max(j_n + 1/2) = 30$ and $n_{\text{DKB}} = 150$. To be conservative, we take an average of two grids for the Fermi model as the final one and estimate the uncertainty by the comparison between different models and grid predictions; however, as one can see from our results, for heavy nuclei the shell model results deviate more and more from those of the Fermi and sphere models, confirming the low applicability of this model for

TABLE I. ΔE_{SE} contribution to the low-lying states to bound-muon energy in units of eV. The next to last column corresponds to our final value with an error bar. The previous results have been taken from Ref. [21] and the one taken from Ref. [22] is noted explicitly.

Ion	State	Shell exp	Shell nonexp	Sphere exp	Sphere nonexp	Fermi exp	Fermi nonexp	Final	Previous
μ^- - ⁹⁰ Zr	$1s_{1/2}$	1169.4	1163.3	1191.6	1180.2	1193.7	1187.7	1191(4)	1218
	$2p_{1/2}$	7.675	7.601	7.055	6.987	7.031	6.963	6.99(5)	1
	$2p_{3/2}$	47.16	47.05	46.59	46.55	46.58	46.47	46.52(6)	41
μ^- - ¹²⁰ Sn	$1s_{1/2}$	1677.6	1665.4	1725.9	1701.0	1729.7	1717.7	1724(7)	
	$2p_{1/2}$	43.61	43.26	40.75	39.86	40.69	40.37	40.5(3)	
	$2p_{3/2}$	123.1	122.7	120.5	119.8	120.5	120.1	120.3(3)	
μ^- - ²⁰⁸ Pb	$1s_{1/2}$	3041.4	3012.0	3229.4	3197.4	3239.4	3210.8	3225(15)	3373 3270(160) [22]
	$2p_{1/2}$	497.6	490.6	457.1	440.9	456.7	450.0	453(5)	413
	$2p_{3/2}$	786.0	779.5	747.8	734.4	747.8	741.5	745(5)	707

heavy muonic atoms. We have also estimated the dependence of our results from the used rms value, and even in the most sensitive case of the $1s_{1/2}$ state it is on the level of 0.1% and well below the nuclear model dependence. The comparison with the current state-of-the-art theoretical predictions from Refs. [21,22] shows disagreement, sometimes even outside of the few-percent uncertainties indicated there, and an order-of-magnitude improvement in the accuracy. However, despite the disagreement in individual contributions, the fine-structure component difference $\Delta 2p$ is in surprisingly good agreement with the earlier predictions, and therefore one can conclude that the last sizable QED effect, namely the SE correction, does not resolve fine-structure muonic anomaly [36]. Finally, the updated rigorous SE results to the transition energies can potentially change the rms values based on the muonic spectra and play an important role in the future for new experiments aiming for the extraction of nuclear moments and rms radii.

Conclusions. We presented rigorous calculations of the SE correction to the few first excited energy levels of muonic atoms and significantly improved results for the ground states, which concludes the leading-order QED predictions. We used three different nuclear charge distributions and two grids to estimate the convergence and uncertainties of our predictions and gave an analytical formula for the Fermi potential

in momentum representation. Theoretical results for low-lying $1s_{1/2}$, $2p_{1/2}$, and $2p_{3/2}$ for muonic zirconium, tin, and lead have been presented and compared with the available published results. Even though in most cases our rigorous calculations agree with the previous mean-value method, sometimes this comparison shows a significant difference between them, therefore justifying the usage of the accurate QED approach for high-precision calculations. More importantly, the rigorous high-precision SE results are an essential part of the state-of-the-art theoretical predictions aiming at a high-precision determination of nuclear radii and other parameters. As for the muonic fine-structure anomaly, for a few decades, it was believed that it could be resolved by accurate predictions for NP or refined SE effects [12,23,25], which is now ruled out. Therefore, even though the renewed SE results do not resolve the fine-structure muonic anomaly, they can affect previous results of the extraction of the nuclear rms radii based on the muonic atoms spectra. Finally, conveniently excluding the long-suggested QED solution to the puzzle stimulates the search for other explanations, including physics beyond the standard model and new experiments with much improved experimental techniques.

Acknowledgments. The author thanks I. A. Valuev, Z. Harman, V. A. Yerokhin, and D. A. Glazov for useful discussions.

- [1] J. A. Wheeler, Some consequences of the electromagnetic interaction between μ^- -mesons and nuclei, *Rev. Mod. Phys.* **21**, 133 (1949).
- [2] E. Borie and G. A. Rinker, The energy levels of muonic atoms, *Rev. Mod. Phys.* **54**, 67 (1982).
- [3] S. Devons and I. Duerdodth, Muonic atoms, in *Advances in Nuclear Physics: Volume 2*, edited by M. Baranger and E. Vogt (Springer US, Boston, MA, 1995), pp. 295–423.
- [4] R. Pohl *et al.*, The size of the proton, *Nature (London)* **466**, 213 (2010).
- [5] C. Piller, C. Gugler, R. Jacot-Guillarmod, L. A. Schaller, L. Schellenberg, H. Schneuwly, G. Fricke, T. Hennemann, and J. Herberz, Nuclear charge radii of the tin isotopes from muonic atoms, *Phys. Rev. C* **42**, 182 (1990).
- [6] L. Schaller, L. Schellenberg, A. Ruetschi, and H. Schneuwly, Nuclear charge radii from muonic x-ray transitions in beryllium, boron, carbon and nitrogen, *Nucl. Phys. A* **343**, 333 (1980).
- [7] T. Y. Saito, M. Niikura, T. Matsuzaki, H. Sakurai, M. Igashira, H. Imao, K. Ishida, T. Katabuchi, Y. Kawashima, M. K. Kubo, Y. Miyake, Y. Mori, K. Ninomiya, A. Sato, K. Shimomura, P. Strasser, A. Taniguchi, D. Tomono, and Y. Watanabe, Muonic x-ray measurement for the nuclear charge distribution: the case of stable palladium isotopes, [arXiv:2204.03233](https://arxiv.org/abs/2204.03233).
- [8] A. Antognini, N. Berger, T. E. Cocolios, R. Dressler, R. Eichler, A. Eggenberger, P. Indelicato, K. Jungmann, C. H. Keitel, K. Kirch, A. Knecht, N. Michel, J. Nuber, N. S. Oreshkina, A. Ouf, A. Papa, R. Pohl, M. Pospelov, E. Rapisarda, N. Ritjoho *et al.*, Measurement of the quadrupole moment of ¹⁸⁵Re and ¹⁸⁷Re from the hyperfine structure of muonic X rays, *Phys. Rev. C* **101**, 054313 (2020).
- [9] W. Dey, P. Ebersold, H. Leisi, F. Scheck, H. Walter, and A. Zehnder, Nuclear spectroscopic ground-state quadrupole

- moments from muonic atoms: The quadrupole moment of ^{175}Lu , *Nucl. Phys. A* **326**, 418 (1979).
- [10] A. Rüetschi, L. Schellenberg, T. Phan, G. Piller, L. Schaller, and H. Schneuwly, Magnetic hyperfine structure in muonic ^{209}Bi , *Nucl. Phys. A* **422**, 461 (1984).
- [11] Y. Tanaka, R. M. Steffen, E. B. Shera, W. Reuter, M. V. Hoehn, and J. D. Zumbro, Precision Muonic-Atom Measurements of Nuclear Quadrupole Moments and the Sternheimer Effect in Rare-Earth Atoms, *Phys. Rev. Lett.* **51**, 1633 (1983).
- [12] P. Bergem, G. Piller, A. Rueetschi, L. A. Schaller, L. Schellenberg, and H. Schneuwly, Nuclear polarization and charge moments of ^{208}Pb from muonic x rays, *Phys. Rev. C* **37**, 2821 (1988).
- [13] C. S. Wu and L. Willets, Muonic atoms and nuclear structure, *Annu. Rev. Nucl. Sci.* **19**, 527 (1969).
- [14] N. Michel, N. S. Oreshkina, and C. H. Keitel, Theoretical prediction of the fine and hyperfine structure of heavy muonic atoms, *Phys. Rev. A* **96**, 032510 (2017).
- [15] A. S. M. Patoary and N. S. Oreshkina, Finite nuclear size effect to the fine structure of heavy muonic atoms, *Eur. Phys. J. D* **72**, 54 (2018).
- [16] N. Michel and N. S. Oreshkina, Higher-order corrections to the dynamic hyperfine structure of muonic atoms, *Phys. Rev. A* **99**, 042501 (2019).
- [17] N. Paul, G. Bian, T. Azuma, S. Okada, and P. Indelicato, Testing Quantum Electrodynamics with Exotic Atoms, *Phys. Rev. Lett.* **126**, 173001 (2021).
- [18] T. Okumura, T. Azuma, D. A. Bennett, P. Caradonna, I. Chiu, W. B. Doriese, M. S. Durkin, J. W. Fowler, J. D. Gard, T. Hashimoto, R. Hayakawa, G. C. Hilton, Y. Ichinohe, P. Indelicato, T. Isobe, S. Kanda, D. Kato, M. Katsuragawa, N. Kawamura, Y. Kino *et al.*, Deexcitation Dynamics of Muonic Atoms Revealed by High-Precision Spectroscopy of Electronic K X Rays, *Phys. Rev. Lett.* **127**, 053001 (2021).
- [19] T. Beier, The g_j factor of a bound electron and the hyperfine structure splitting in hydrogenlike ions, *Phys. Rep.* **339**, 79 (2000).
- [20] R. Barrett, Radiative corrections in muonic atoms, *Phys. Lett. B* **28**, 93 (1968).
- [21] A. Haga, Y. Horikawa, and H. Toki, Reanalysis of muonic ^{90}Zr and ^{208}Pb atoms, *Phys. Rev. C* **75**, 044315 (2007).
- [22] K. T. Cheng, W.-D. Sepp, W. R. Johnson, and B. Fricke, Self-energy corrections in heavy muonic atoms, *Phys. Rev. A* **17**, 489 (1978).
- [23] T. Q. Phan, P. Bergem, A. Rüetschi, L. A. Schaller, and L. Schellenberg, Nuclear polarization in muonic ^{90}Zr , *Phys. Rev. C* **32**, 609 (1985).
- [24] Y. Yamazaki, H. D. Wohlfahrt, E. B. Shera, M. V. Hoehn, and R. M. Steffen, Discrepancy between Theory and Experiment in Nuclear Polarization Corrections of Muonic ^{208}Pb , *Phys. Rev. Lett.* **42**, 1470 (1979).
- [25] I. A. Valuev, G. Colò, X. Roca-Maza, C. H. Keitel, and N. S. Oreshkina, Evidence Against Nuclear Polarization as Source of Fine-Structure Anomalies in Muonic Atoms, *Phys. Rev. Lett.* **128**, 203001 (2022).
- [26] G. E. Brown, J. S. Langer, and G. W. Schaefer, Lamb shift of a tightly bound electron I. Method, *Proc. R. Soc. A* **251**, 92 (1959).
- [27] A. M. Desiderio and W. R. Johnson, Lamb shift and binding energies of K electrons in heavy atoms, *Phys. Rev. A* **3**, 1267 (1971).
- [28] P. J. Mohr, Self-energy of the $n = 2$ states in a strong Coulomb field, *Phys. Rev. A* **26**, 2338 (1982).
- [29] P. Indelicato and P. J. Mohr, Coordinate-space approach to the bound-electron self-energy, *Phys. Rev. A* **46**, 172 (1992).
- [30] V. A. Yerokhin and V. M. Shabaev, First-order self-energy correction in hydrogenlike systems, *Phys. Rev. A* **60**, 800 (1999).
- [31] N. S. Oreshkina, H. Cakir, B. Sikora, V. A. Yerokhin, V. Debierre, Z. Harman, and C. H. Keitel, Self-energy-corrected Dirac wave functions for advanced QED calculations in highly charged ions, *Phys. Rev. A* **101**, 032511 (2020).
- [32] N. J. Snyderman, Electron radiative self-energy of highly stripped heavy atoms, *Ann. Phys. (NY)* **211**, 43 (1991).
- [33] F. A. Parpia and A. K. Mohanty, Relativistic basis-set calculations for atoms with Fermi nuclei, *Phys. Rev. A* **46**, 3735 (1992).
- [34] V. M. Shabaev, I. I. Tupitsyn, V. A. Yerokhin, G. Plunien, and G. Soff, Dual Kinetic Balance Approach to Basis-Set Expansions for the Dirac Equation, *Phys. Rev. Lett.* **93**, 130405 (2004).
- [35] QUADPACK, <http://www.netlib.org/quadpack/>.
- [36] The absolute value of the anomaly, i.e., the difference between the experiment and theory, is estimated to be about 20(8) eV for muonic zirconium [23], 150(20) eV for muonic tin [5], and 324(27) eV for muonic lead [12].